Vacancy defects in *p*-type 6*H*-SiC created by low-energy electron irradiation

H. J. von Bardeleben,[1] J. L. Cantin,[1] L. Henry,[2] and M. F. Barthe[2]
[1]*Groupe de Physique des Solides, Universités Paris 6&7, UMR 75-88 au CNRS, Tour 23, 2 Place Jussieu, 75251 Paris Cedex 05, France*
[2]*Centre d'Etudes et de Recherches par Irradiation, CNRS, 45071 Cedex 02, Orléans, France*

(Received 5 April 2000)

The intrinsic defects in *p*-type 6*H*-SiC:Al generated by electron irradiation at 300 keV, which is close to the threshold of the silicon atom displacement, have been studied by electron paramagnetic resonance spectroscopy. We observed two dominant irradiation-induced paramagnetic defects: (i) a silicon-vacancy-related spin $S=3/2$ defect with a zero-field splitting of $D=68.7\times10^{-4}$ cm^{-1}, which is tentatively attributed to a Si Frenkel pair aligned parallel to the *c* axis and (ii) a carbon-vacancy-related spin $S=1/2$ defect already previously attributed to $V_C{}^+$. A slight increase of the electron energy to 350 keV creates in addition a lower-symmetry $S=3/2$ spectrum equally attributed to Si Frenkel pairs with the interstitial being located at six equivalent off-axis sites. High-energy irradiation (2 MeV) creates only isolated Si vacancies with no zero-field splitting.

INTRODUCTION

Intrinsic defects in 6*H*-SiC have been observed by electron paramagnetic resonance (EPR) and positron annihilation spectroscopy after thermal treatments,[1] electron and neutron irradiation,[2–7] and ion implantation.[8–10] The EPR studies have revealed a complex situation with numerous spin $S=\frac{1}{2}$, 1, and $\frac{3}{2}$ defects, the last characterized by widely varying crystal field splittings. Two models, divacancy centers[1,4] and Frenkel pairs[7] with different pair separations and orientation have been tentatively proposed but their attribution is still unclear. A convincing identification of the microscopic structure of intrinsic defects in SiC-6*H* has only been achieved in two cases: the negatively charged Si vacancy in the high-spin state $S=\frac{3}{2}$,[5] and more recently the positively charged carbon vacancy.[6,7] The models are based on the analysis of the first- and second-nearest-neighbor hyperfine interactions, which are directly resolved in their EPR spectra. The spin of the $V_{Si}{}^-$ center could not be determined from the EPR spectrum as no zero-field splitting was observed in spite of the C_{3v} symmetry of the Si sites in 6*H*-SiC. Its spin $S=\frac{3}{2}$ ground state was only obtained from an additional electron nuclear double resonance (ENDOR) study. The $V_{Si}{}^-$ and $V_C{}^+$ defects do not show any site dependence in their EPR spectra. All of these studies have been performed on samples irradiated with high-energy (>MeV) particles, where vacancies and dissociated interstitials are the primary defects.

Whereas vacancy and antisite defects have been studied in most of the IV, II-VI, and III-V semiconductors, interstitial-related defects have been observed only in rare cases; SiC is not an exception and no results on the electronic structure and thermal stability of the carbon and silicon interstitials have been obtained. This is generally attributed to their strong tendency to form associated defects, combined with a high mobility even at cryogenic temperatures. The simplest interstitial-associated defect is the Frenkel pair, which can be generated in a controlled way by electron irradiation close to the threshold energy for single-atom displacement. In spite of being the primary irradiation defect, Frenkel pairs up to now have not been observed in the main semiconductor materials and only one case—V_{Zn}-Zn_i in ZnSe—has been well evidenced by magnetic resonance spectroscopy.[11,12]

We report here the results of an EPR study of the defects generated by low-energy electron irradiation, which leads to the formation of close Frenkel pairs as primary defects. Indeed, if the electron energy is close to the displacement threshold for an atom displacement, the displaced atom has not sufficient kinetic energy to diffuse away from the vacancy site. For 6*H*-SiC the displacement energy E_d for C and Si atoms has been estimated as $T_d=23$ eV;[13] this value was obtained from radiative lifetime measurements in light-emitting diodes irradiated with electrons in the 100 keV to 1 MeV range. Displacement energies E_D of 20 and 30 eV can be considered as reasonable limiting lower and upper values. The corresponding electron energies necessary for C and Si atom displacement are shown in Fig. 1: 100 and 150 keV for C atoms and 220 and 300 keV for Si atoms. The minimum energies required to displace a C or Si atom are different due to the mass difference between carbon and silicon atoms ($M_{Si}/M_C=2.33$), which determines the maximum energy that can be transmitted in the elastic collision between the electron and the lattice atom. In addition, the transmitted energy depends equally on the recoil angle and is maximum for head-on collisions; thus, a preferential alignment parallel to the electron beam direction of the vacancy-interstitial pairs is expected under threshold irradiation conditions.

We have studied the effect of electron irradiation at 300 keV in *p*-type Al-doped 6*H*-SiC bulk samples. For this energy the expected primary radiation defects are spatially separated carbon vacancies and carbon interstitials and close silicon Frenkel pairs. The thermal stability of the Si Frenkel pair will of course depend on a number of parameters, such as irradiation temperature, beam current, and postirradiation annealing. To optimize the conditions for their observation we have irradiated the samples at low temperature (77 K) and under moderate beam currents (<10 μA/cm^2). We have

 ©2000 The American Physical Society

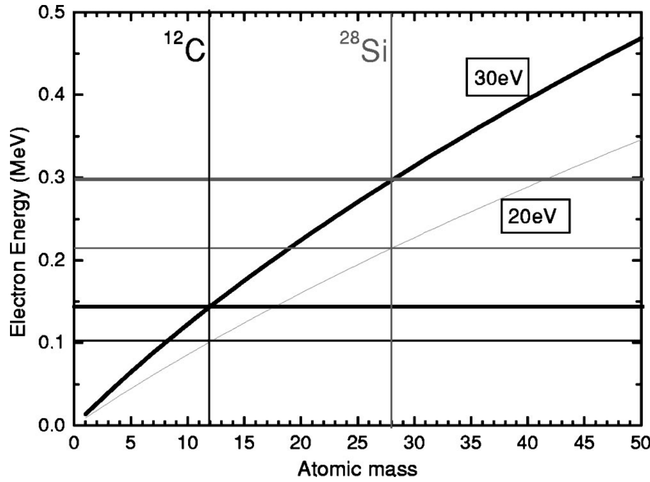

FIG. 1. Minimal electron energies required to transmit either 20 or 30 eV to an atom of atomic mass A in an elastic collision. In the case of a displacement energy of 30 eV, electron energies of, respectively, 150 and 300 keV are required for C and Si displacements.

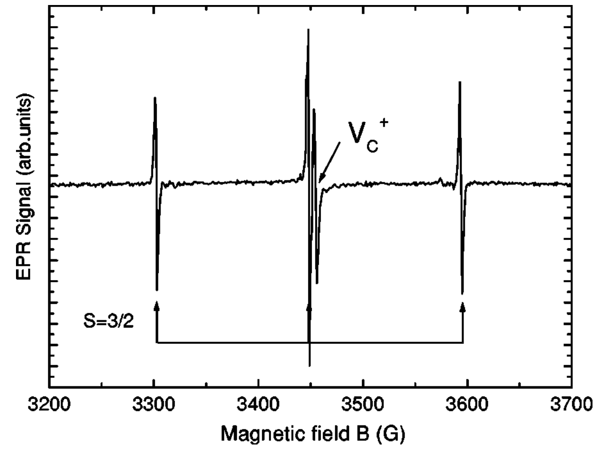

FIG. 2. EPR spectrum of $6H$-SiC:Al irradiated with 300 keV electrons to a dose of $2\times10^{18}\,\mathrm{cm}^{-2}$, measured for $B\|[0001]$ at $T=300\,\mathrm{K}$, $f=9.659\,\mathrm{GHz}$. It displays the spectra of the spin $S=3/2$ V_{Si}^{-}-X center and the V_{C}^{+} center.

also investigated the case of slightly higher electron energy (350 keV) and a high energy of 2 MeV.

EXPERIMENT

The samples were commercially purchased 300-μm-thick p-type Al-doped ($3.7\times10^{18}\,\mathrm{cm}^{-3}$) $6H$-SiC, wafers. Typical sample dimensions are 5×5 mm. The electron irradiation was performed at 77 K with the electron beam parallel to the c axis. Typical beam currents were 5 μA/cm^2; the total doses ranged from 5×10^{17} to $2\times10^{18}\,\mathrm{cm}^{-2}$. The X-band EPR measurements were performed in the 4–300 K temperature range. The g factors were determined with a precision of $\Delta g\approx\pm0.0001$ via a microwave frequency counter and calibration of the magnetic field by a proton NMR probe. The angular variation of the EPR spectra was measured for a rotation of the magnetic field in the $(11\bar{2}0)$ and (0001) planes.

RESULTS

After irradiation with a dose of $\geqslant1\times10^{18}\,\mathrm{cm}^{-2}$ two different EPR spectra are observed (Fig. 2) at room temperature. Due to their widely different linewidths (2 G vs 300 mG) they can be easily distinguished. The first one is a spin $S=\frac{1}{2}$ spectrum with g values $g_{xx}=1.9962$, $g_{yy}=2.0019$, $g_{zz}=2.0015$ with the principal axes of the g tensor inclined $\theta=40.6°$ from the c axis in the $(11\bar{2}0)$ plane. This spectrum has already previously been observed after 2.5 MeV electron irradiation and has been attributed to the positively charged carbon vacancy V_{C}^{+}.[6,7] It will not be further discussed here. The second EPR spectrum, which is the main object of this paper, is characterized by an anisotropic three-line spectrum of axial symmetry (Fig. 3). Its angular variation has been measured for a rotation of the magnetic field in the $(11\bar{2}0)$ and (0001) planes. It is described by the spin Hamiltonian

$$H=\mu_B SgB+SDS+\sum_j SA_jI_j,$$

in which the symbols have their usual meanings (see Ref. 5 for more details). The Zeeman and fine structure parameters follow: electron spin $S=\frac{3}{2}$, g values $g_{\|c}=2.0032\pm0.0001$, $g_{\perp c}=2.0028\pm0.0001$, and a zero-field splitting of $D=68.7\times10^{-4}\,\mathrm{cm}^{-1}$. The spectrum has axial symmetry around the [0001] axis. The hyperfine interaction parameters are given in Table I. The angular variation of the resonance position of the central $|\pm\frac{1}{2}\rangle$ line (Fig. 4) has been resolved and the good agreement with the simulated variation further confirms the spin $S=\frac{3}{2}$ of the defect. The effective introduction rate for this defect is $\sim10^{-1}\,\mathrm{cm}^{-1}$.

More information on the microscopic structure of this defect has been obtained from analysis of the Si and C hyperfine (HF) interactions for which the intensity and angular variations have been measured. Each of the three fine structure lines is accompanied by nearest-(NN) and next-nearest-neighbor (NNN) hyperfine interaction. The superhyperfine (SHF) interaction structure is best resolved for the central line, as the $|\pm\frac{3}{2}\rangle\rightarrow|\pm\frac{1}{2}\rangle$ lines are sensitive to local variation in the crystal field parameter D. The peak-to-peak linewidth

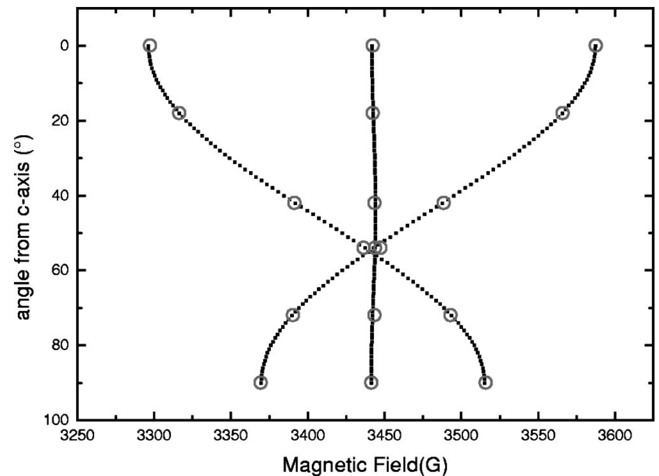

FIG. 3. Experimental (circles) and simulated (dots) angular variation of the three allowed ($\Delta M=\pm1$) fine structure transitions of the $S=3/2$ spectrum; rotation plane $(11\bar{2}0)$, $T=300\,\mathrm{K}$, $f=9.650\,\mathrm{GHz}$.

TABLE I. In the first section, the spin, g factor, and zero field splitting parameter D are given; the second and third sections show the superhyperfine interaction tensors with the 4 NN carbon and the 12 NN silicon atoms.

	3C-SiC	6H-SiC:N	6H-SiC:Al
Spin	3/2	3/2	3/2
g factor	2.0029	2.0015[a]	$g\parallel c = 2.0032$
			$g\perp c = 2.0028$
D (10^{-4} cm^{-1})	0	0	68.7
		Number of atoms	
	4C NN	4C NN	3C NN
$T_{\parallel \mathrm{NN}}$(C) (G)	28.6	28.8	28.6
$T_{\perp \mathrm{NN}}$(C) (G)	11.8	11.6	13.3
			1C NN
$T_{\parallel c}$(C) (G)			28.5
$T_{\perp c}$(C) (G)			17.2
	12Si NNN	12Si NNN	3Si NNN
T_{iso}(Si) (G)	2.92	2.98	3.84
T_{iso}(Si) (G)			3.52
			6Si NNN
T_{iso}(Si) (G)			2.53
Model	$V_{\mathrm{Si}}{}^{-}$	$V_{\mathrm{Si}}{}^{-}$	$V_{\mathrm{Si}}{}^{-}$-Si
Reference	3	5	This work

[a]The g value of 2.0015 must be erroneous; our measurements on the isolated Si vacancy obtained after high-energy electron or proton irradiation show an isotropic g value of 2.0032.

of the central line is 300 mG. The highest-intensity HF lines (Fig. 5) are two doublets of nearly equal amplitude, different linewidths 300 and 400 mG, and isotropic splittings of 2.5 and 3.5 G, respectively. The apparent higher linewidth of the outer doublet is attributed to the superposition of two nonresolved HF doublets. Indeed, assuming equal linewidths of 300 mG the SHF structure can be excellently simulated by the sum of three doublets with intensities 2:1:1 and splittings of 2.53, 3.52, and 3.84 G, respectively. A double integration

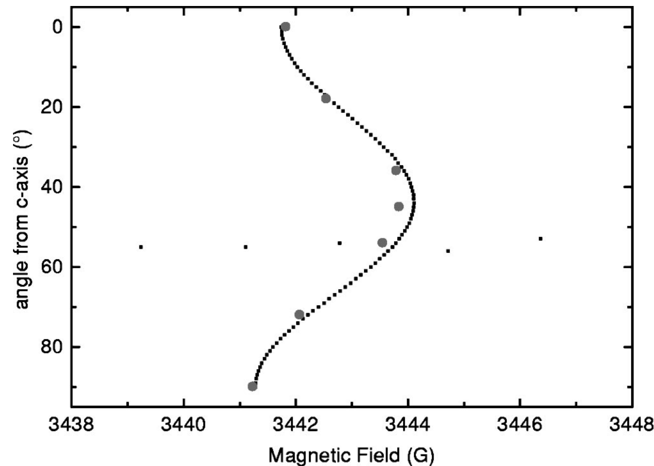

FIG. 4. Experimental (circles) and simulated (dots) angular variation of the central line of the $S = 3/2$ spectrum; rotation plane $(11\bar{2}0)$, $T = 300$ K, $f = 9.650$ GHz.

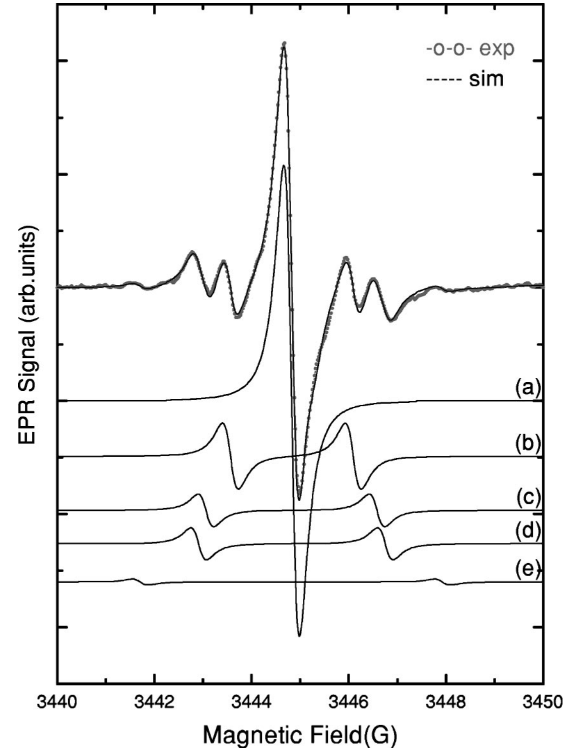

FIG. 5. Experimental EPR spectrum (dots) and simulated spectrum (line) of the central part of the $V_{\mathrm{Si}}{}^{-}$ spectrum for $B \parallel [0001]$, $f = 9.659$ GHz. Below are shown the different components of the simulation: (a) central line without hyperfine interaction, (b) superhyperfine interaction with one ^{29}Si nucleus located in a shell of six equivalent atoms, (c) and (d) SHF interaction with one ^{29}Si nucleus located in two shells of three equivalent atoms, and (e) SHF interaction with two ^{29}Si nuclei in the NNN shell.

gives in this case an intensity ratio relative to the central line of (0.141,0.070,0.070), which is characteristic for an interaction with shells composed of six, three, and three Si neighbors, respectively (Fig. 5). The theoretical ratios corresponding to the 4.7% abundance of ^{29}Si are 0.146/0.0713/0.0713. The additional weaker lines [Fig. 5(e)] correspond to the presence of two ^{29}Si in the neighbor shells. The three set of SHF doublets are attributed to the six NNN Si atoms in the (0001) plane of the vacancy and the three NNN Si atoms above and below this plane. In the case of the isolated vacancy $V_{\mathrm{Si}}{}^{-}$, these 12 silicon sites have been found[5] to be indistinguishable.

At higher gain a second set of hyperfine lines with larger splittings is observed (Fig. 6): for $B \parallel [0001]$ it is composed of two doublets with intensity ratio 1:3 and splittings of 28.6 and 15.0 G, respectively. This HF interaction is anisotropic and has axial symmetry around the nearest-neighbor directions. The intensity ratios of the HF lines to the central line are 5.5×10^{-3}:1 and 1.5×10^{-2}:1, demonstrating interaction with one and three C atoms. Detailed study of the angular variation of these HF lines (Fig. 7) shows that the four C atoms are not equivalent but have slightly different HF tensors for the C atom on the c axis and the three C atoms in the (0001) plane. The ^{13}C and ^{29}Si hyperfine interactions with (3+1) C and (6+3+3) Si atoms are characteristic of a Si site defect.

The numerical values of the g factor and HF interactions

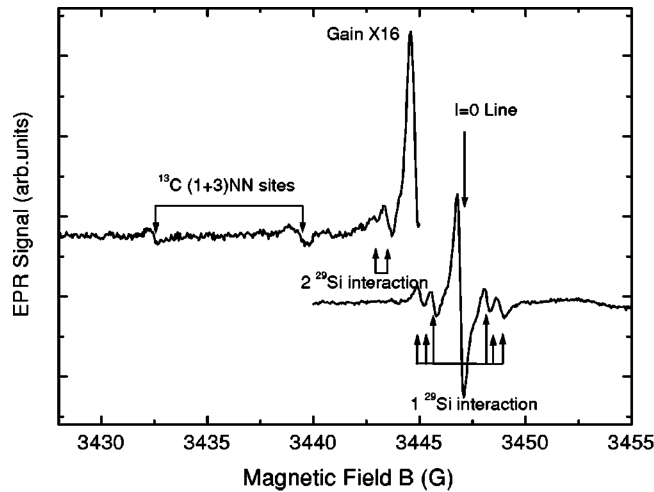

FIG. 6. High-gain EPR spectrum of the $V_{Si}{}^{-}$-X center displaying in addition to the ^{29}Si SHF lines the ^{13}C hyperfine lines; $B \| [0001]$, $T=300$ K, $f=9.664$ GHz.

are compared in Table I with those previously determined for the negative Si vacancy observed after high-energy irradiation in $3C$-SiC and n-type $6H$-SiC. From the components of the axial HF tensor A the isotropic (a) and anisotropic (b) dipolar parts can be deduced: $a=(A_{\|}+2A_{\perp})/3$ and $b=(A_{\|}-A_{\perp})/3$. The numerical values of the isotropic (a) and dipolar (b) components of the HF interaction tensors are close to the ones predicted for the isolated $V_{Si}{}^{-}$ defect in $3C$-SiC; they differ from the ones observed previously for the isolated $V_{Si}{}^{-}$ in high-energy-irradiated $6H$-SiC: for the ^{13}C hyperfine tensors of the two types of C NN atom we obtain values of $a_1=18.4$ G, $b_1=5.1$ G, and $a_2=21.0$ G, $b_2=3.8$ G as compared to the calculated values[5] of $a=25.5$ G and $b=4.2$ G. The theoretical value for the NNN ^{29}Si HF interaction is $a=2.56$ G, which has to be compared to the experimental values of 2.53, 3.52, and 3.84 G for the three sets of Si atoms.

We attribute this defect from its spin Hamiltonian parameters and in agreement with the threshold irradiation conditions to the negatively charged silicon vacancy $V_{Si}{}^{-}$ associated with a second defect. Unlike the $V_{Si}{}^{-}$ defect observed previously in n-type $6H$-SiC after high-energy electron or particle irradiation, the zero-field splitting of its $^4A_2$ ground state demonstrates directly the presence of a second associated defect located in the [0001] direction relative to the Si vacancy. In order to further clarify the origin of the splitting we have similarly irradiated a cubic polytype $3C$-SiC:B sample with 300 keV electrons. In this sample the same EPR spectrum, with in particular the same fine structure D value, as in p-type $6H$-SiC is observed. This result demonstrates that the origin of the D term must be related to the fact that the center is not the isolated silicon vacancy but a Si-vacancy–pair defect.

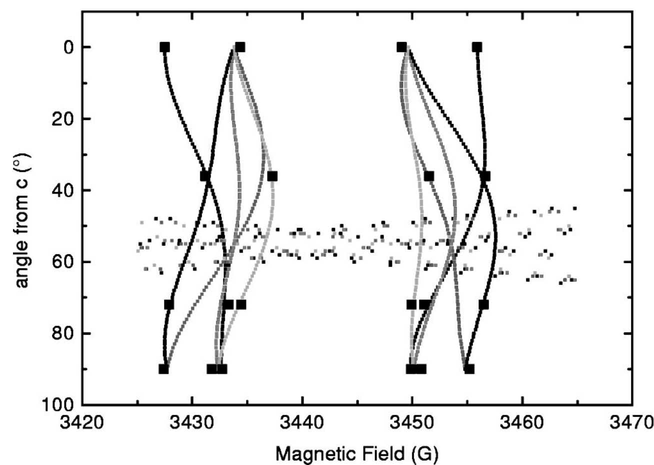

FIG. 7. Experimental (squares) and simulated angular variation of the ^{13}C HF lines; rotation plane $(11\bar{2}0)$, $T=300$ K, 9.648 GHz.

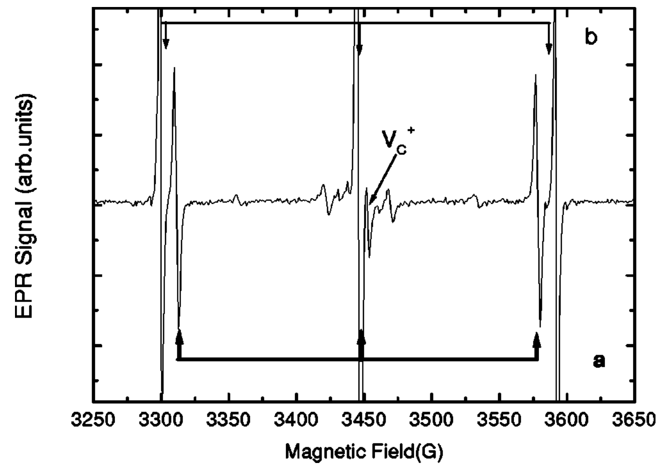

FIG. 8. EPR spectrum of $6H$-SiC:Al after a 350 keV electron irradiation; $B \| c$, $T=300$ K, $f=9.659$ GHz. In addition to the $S=3/2$ $V_{Si}{}^{-}$-X (b) and $S=1$ $V_C{}^{+}$ spectra observed after 300 keV electron irradiation, an additional $S=3/2$ spectrum (a) is observed; the central lines of the two $S=3/2$ spectra are not distinguished for this magnetic field scale but can be decomposed at higher resolution (Fig. 9 below).

Under the irradiation conditions chosen here the Si-sublattice-related primary radiation defects are Si Frenkel pairs, preferentially aligned parallel to the c axis, and we will thus consider this model for the $V_{Si}{}^{-}$-X defect with X being a Si interstitial atom. The alignment of this defect pair parallel to the electron beam direction is also a very strong indication of it being a primary defect generated under displacement threshold conditions. Indeed, in the electron–lattice-atom collision the electrons of mass m transmit a maximum energy T_m to a lattice atom of mass M for head-on collisions. For other recoil angles φ the transmitted energy is smaller and varies as $T=T_m \cos^2 \varphi$. Whereas at high electron energies sufficient energy for displacement of the lattice atom is transmitted for all impact angles, near the threshold only head-on collision will be possible with the interstitial displaced parallel to the beam direction, [0001] in our case.

In order to further verify this model we have investigated in more detail the effect of the electron energy on this defect structure. The increase of the electron energy from 300 to 350 keV leads to the formation of an additional—lower-intensity—$S=\frac{3}{2}$ defect spectrum with a different defect orientation (Fig. 8). The distinction between a spin $S=\frac{3}{2}$ and a $S=1$ center from its EPR spectrum is in general not straightforward in SiC, if we have the simultaneous presence of an additional spin $S=\frac{1}{2}$ or $\frac{3}{2}$ center with a similar g value; this is the case here. However, a decomposition of the central part

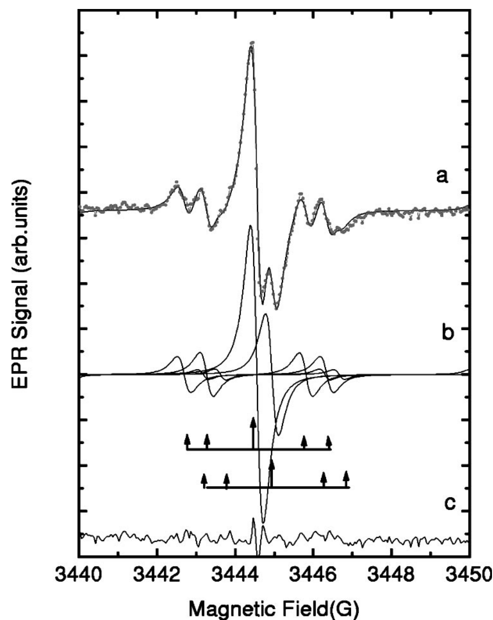

FIG. 9. Central part of the EPR spectrum at $f=9.659$ GHz after 350 keV-electron irradiation. The experimental spectrum [(a) dots] is decomposed into the sum of two central lines with their characteristic ^{29}Si SHF lines from the 2^{Nd} NN shells (b); the resulting sum spectrum is shown in [(a) line]; the difference spectrum between the experimental and the total simulated spectra is given in (c).

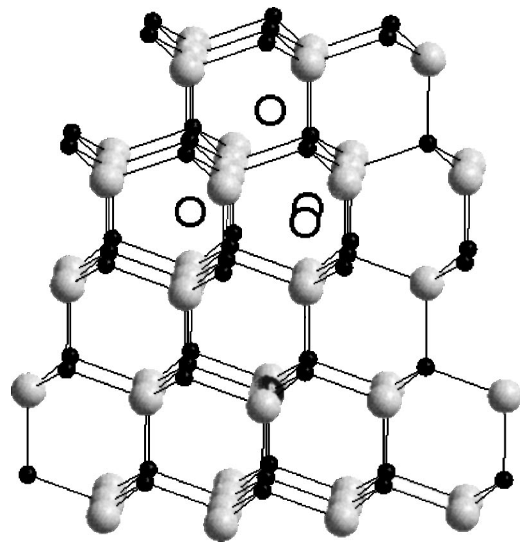

FIG. 11. Model of the silicon Frenkel pair configurations in 6H-SiC (Si and C atoms are represented, respectively, by large gray and small black circles). The Si vacancy (black large circle) is on a quasicubic $c2$ site. The one on-axis and the three 24° off-axis possible Si interstitial positions of T_d symmetry are represented (open circles). The distances are, respectively, 6.5 and 4.5 Å. Depending on the vacancy sites, the 24° off-axis interstitial sites are rotated by 60°.

of the spectrum allows one for $B\|c$ to resolve clearly two central lines with identical Si NNN SHF structure; it confirms the $S=\frac{3}{2}$ character of the additional defect (Fig. 9). From the angular variation (Fig. 10) the spin Hamiltonian parameters are determined to be $g_{xx}=2.0015$, $g_{yy}=2.0039$, $g_{zz}=2.0035$ with $\Delta g=\pm 0.0005$, and zero-field splitting parameters $D=76\times 10^{-4}\,\mathrm{cm}^{-1}$ and $E=19\times 10^{-4}\,\mathrm{cm}^{-1}$ with the z axis of the fine structure tensor aligned 24° from the c axis in the $(11\bar{2}0)$ plane. We attribute this additional defect from the special irradiation conditions leading to its formation and the similarity of the numerical values of the spin

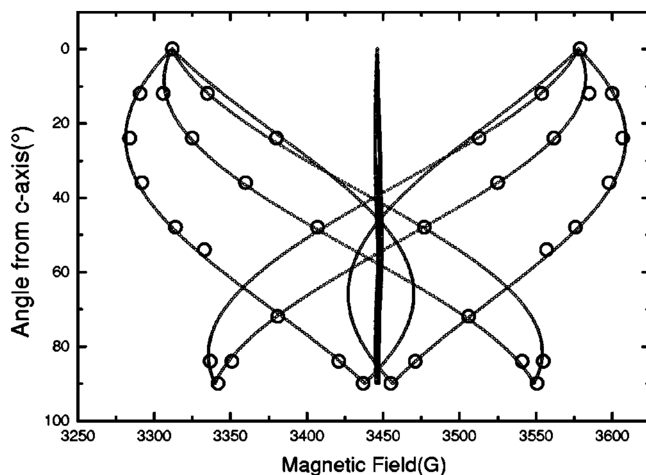

FIG. 10. Experimental (circles) and simulated angular variation of the three allowed fine structure transitions ($\Delta M=\pm 1$) of the additional $S=3/2$ spectrum observed after 350 keV electron irradiation, shown as (a) for $B\|[0001]$ in Fig. 8; rotation plane $(11\bar{2}0)$, $T=300$ K, $f=9.659$ GHz.

Hamiltonian parameters to a differently orientated V_{Si}-Si_i pair. The six equivalent orientations of these ''24°'' Frenkel pairs and their axis orientations allow us to locate the interstitial Si atom relative to the V_{Si} site (Fig. 11). Each of the three quasicubic and hexagonal Si sites is surrounded by three interstitial sites of T_d symmetry oriented at 24° from the c axis and at a distance of 4.5 Å. An interstitial lattice site of the same symmetry is also present on the c axis at 6.5, 3.7, and 1.6 Å from, respectively, the quasicubic-2, hexagonal, and quasicubic-1 Si vacancy sites. As only one configuration for the on-axis center is observed, it must be assumed that the close configurations are not stable relative to a recombination or that their observation depends on the Fermi level position. The influence of the Si energy threshold value and the preferential electron beam parallel alignment leave no doubt that the interstitial atom is Si. For high-energy (2 MeV) electron irradiation, the two $V_{\mathrm{Si}}{}^{-}$-X centers discussed here are no longer observed and only the isolated $V_{\mathrm{Si}}{}^{-}$ defect, previously reported, is detected.

DISCUSSION

The attribution of the spin $S=\frac{3}{2}$ centers observed in this work to Si vacancy defect complexes is based on the numerical values and intensities of the resolved superhyperfine interactions with the C and Si neighboring shells, which are well known from theory and previous experimental results. The lower symmetry deduced from the anisotropy of the g tensor and presence of a zero-field splitting distinguishes the centers observed here from those reported in previous studies. We clearly observe a defect complex. The formation conditions for these complexes—Si threshold electron energies—are unique. In spite of many different irradiation conditions employed in the previous EPR studies, a $V_{\mathrm{Si}}{}^{-}$

complex has never been observed before to our knowledge: in these cases high-energy electron or particle irradiation has been used, in which sufficient energy is transmitted to the displaced atoms to separate them from the primary vacancy. Under these conditions the formation of isolated V_{Si}^- silicon vacancies with an apparent T_d symmetry is expected and observed; secondary defect complexes might also be expected but have not yet been identified. The V_{Si}^- defect observed here is unique and related to the fact that the energy of the electron irradiation is close to the threshold for Si atom displacement, i.e., the proximity of the displaced Si atom from its primary vacancy.

It might seem surprising that the interstitial Si atom is not directly observed in the EPR experiment. It should be recalled, however, that direct observability will depend on the presence of a paramagnetic ground state. The Si interstitial is expected to be diamagnetic for the 0 and $+2$ charge states and paramagnetic in the -1 and $+1$ states. The situation seems to be close to that of ZnSe, the only case where a Frenkel pair has been observed previously. In ZnSe also, the presence of the interstitial Zn atom of the V_{Zn}-Zn_i pair is in the EPR experiment only noticed by a change in the spin Hamiltonian parameters as compared to those of the isolated vacancy. The interstitial is in a diamagnetic ground state and only directly observable in optically detected magnetic resonance experiments via its excited states. A simple model relating the site symmetry and charge state for the interstitial has been developed by Watkins.[14] According to his model, in which the $s^m p^n$ electron configuration of the interstitial atom is correlated with the site symmetry, a charge state of $+2$ with a diamagnetic ground state is expected for a T_d interstitial site, which is compatible with the model proposed here. A second interaction that could give rise to an EPR observation of the Si interstitial is the SHF interaction of the 4.7% abundant ^{29}Si nuclei, if it is sufficiently strong as compared to the linewidth of the spectrum. Indeed, the SHF interaction with the nearest- (C) and next-nearest-neighbor (Si) shells is resolved in the EPR spectrum. The SHF interaction is usually decomposed into isotropic and anisotropic parts, which are related to the wave function extension and the defect pair distance, respectively. The isotropic character of the resolved ^{29}Si NNN interaction demonstrates that the dipolar contribution at this distance is already negligible. In the microscopic model proposed here, the on-axis interstitial is located at 6.5 Å from the V_{Si} site and the off-axis interstitials at 4.5 Å. As both distances are greater than the second-nearest-neighbor distance V_{Si}-Si_{Si} of 3.1 Å, the dipolar SHF interaction will also be negligible for the even more distant interstitial Si atom. The evaluation of the contribution of the isotropic part is not possible without detailed modeling of the defect structure. Our experimental results indicate values of the SHF interaction of the interstitial Si equal to or smaller than the Si NNN interaction. We have, of course, attempted to detect this interaction by a thorough analysis of the SHF structure of the central line of the spectrum, which has the smallest linewidth of the three fine structure transitions. However, the presence of three different ^{29}Si SHF sets as well as the additional structures from these sets when occupied by more than one ^{29}Si atom render further decompositions not sufficiently reliable. The complications due to the overlap of the SHF structures might be overcome by additional ENDOR studies, which, due to their higher resolution, are expected to resolve such weak interactions.

CONCLUSION

In conclusion, we have observed in p-type $6H$-SiC, irradiated with electrons of low energy close to the threshold for silicon atom displacement, two silicon-vacancy-related defects, which are attributed to on-axis and 24° off-axis Si Frenkel pairs V_{Si}^--Si_i.

ACKNOWLEDGMENT

We thank LETI/CEA (Grenoble) for supporting this work.

[1] V. S. Vainer and V. A. Il'in, Fiz. Tverd. Tela (Leningrad) **23**, 3482 (1982) [Sov. Phys. Solid State **23**, 2125 (1981)].
[2] L. A. de S. Balona and J. H. Loubser, J. Phys. C **3**, 2344 (1970).
[3] H. Itoh, N. Hayakawa, I. Nashiyama, and E. Sakuma, J. Appl. Phys. **66**, 4529 (1989).
[4] N. M. Pavlov, M. I. Iglitsyn, M. G. Kosaganova, and V. N. Solomatin, Fiz. Tekh. Poluprovodn **9**, 1279 (1975) [Sov. Phys. Semicond. **9**, 845 (1975)].
[5] T. Wimbauer, B. K. Meyer, A. Hofstätter, A. Scharmann, and H. Overhof, Phys. Rev. B **56**, 7384 (1997).
[6] N. T. Son, W. M. Chen, J. L. Lindström, B. Monemar, and E. Janzen, Mater. Sci. Forum **264–268**, 599 (1998).
[7] D. Cha, H. Itoh, N. Morishita, A. Kawasuso, T. Oshshima, Y. Watanabe, J. Ko, K. Lee, and I. Nashiyama, Mater. Sci. Forum **264–268**, 615 (1998).
[8] S. Dannefaer, D. Craigen, and D. Kerr, Phys. Rev. B **51**, 1928 (1996).
[9] G. Brauer, W. Anwand, P. G. Coleman, A. P. Knights, F. Plazola, Y. Pacaud, W. Skorupa, J. Störmer, and P. Willutzki, Phys. Rev. B **54**, 3084 (1996).
[10] G. Brauer, W. Anwand, E. M. Nicht, J. Kuriplach, M. Sob, N. Wagner, P. G. Coleman, M. J. Puska, and T. Korhonen, Phys. Rev. B **54**, 2512 (1996).
[11] G. D. Watkins, Phys. Rev. Lett. **33**, 223 (1974).
[12] F. Rong and G. D. Watkins, Phys. Rev. Lett. **56**, 2310 (1986).
[13] A. L. Barry, B. Lehmann, D. Fritsch, and D. Braunig, IEEE Trans. Nucl. Sci. **38**, 1111 (1991).
[14] G. D. Watkins, in *Material Science and Technology*, edited by W. Schröter, Vol. 4 (VCH, Weinheim, 1991), p. 105.